Advances in Machinery, Materials Science and Engineering Application
M. Chen et al. (Eds.)

doi:10.3233/ATDE220437

High Throughput Preparation of Inconel 718 Alloy with Different Nb Content Based on 3D Printing

Liang ZHANG [a,1], Lin LU and Qiyun YANG [a]
[a] *Shanghai Engineering Research Center of 3D Printing Materials, Shanghai Research Institute of Materials, Shanghai 200437, China*

Abstract. Using high throughput method of 3D printing, 20 Inconel 718 alloy samples with different Nb contents (0~10 wt.%) are conveniently prepared in a single printing process, and then analyzed the microscopic morphology and hardness of these samples. The results show that with the increase of Nb content in the alloy, the content of Laves phase in the alloy gradually increases, and the Laves phase particles also become larger, resulting in a gradual increase in hardness. In conclusion, the new technology breaks disadvantages of traditional new material development such as high cost, long time consuming, single trial and error, and provides the possibility for rapid and accurate development of new materials.

Keywords. Inconel 718 alloy, high throughput, 3D printing

1. Introduction

Today, the research and development level of new materials is the premise, forerunner and support for the development of all high and new technologies. However, the current material design methods and systems make the design cycle of new materials long, and the success rate is low, material properties have gradually failed to meet the harsh requirements of current product design, become the core bottleneck restricting the improvement of comprehensive performance of products. Taking aerospace materials as an example, the time period from development to application of nickel-based superalloys is as high as 8-10 years per generation [1-6]. Under the restriction of such a long research and development period, the development of new superalloys has led to serious limitations in the design and development of high performance aeroengines.

In the view of above question, this study firstly designs a double channel powder feeder to achieve the uniform and quantitative mixing of two kinds of powder [1, 7]. On this basis, a high throughput fabrication technology based on additive manufacturing is developed. Using this new technique, 20 nickel-based superalloy samples with different Nb contents (0~10 wt.%) are prepared in a single printing process, and then analyzed the microscopic morphology and hardness of these samples. Finally, combined with the material optimization screening technology, the high-throughput controllable preparation and optimal screening of materials are realized, which breaks the traditional

---

[1] Liang Zhang, Corresponding author, Shanghai Engineering Research Center of 3D Printing Materials, Shanghai Research Institute of Materials, Shanghai 200437, China; E-mail: lzhang0126@hotmail.com.

method of high cost, long time consuming and single experiment trial and error in the development of new materials.

2. Experimental Procedures

Ni-based superalloy block samples with different Nb contents (0~10 wt.%) are prepared by high throughput method of additive manufacturing [7-9]. The specific steps are as follows: (1) Two kinds of spherical nickel-based superalloy powder containing different Nb contents, powder A (1.03wt.% Nb) and powder B (7.98wt.% Nb), are prepared by vacuum gas atomization; (2) The sieved Inconel 718 nickel-base superalloy powders A and B with slightly different compositions are placed into two independent powder conveying systems connected by a tee; (3) Adjust the rotary speed of the powder conveying system to achieve the specific ratio of 0% powder A+100% powder B in the mixed powder. The mixed powder is transported to the laser processing area by inert gas argon; (4) The laser power is set in the range of 1500~2000 W and the laser speed is set in the range of 5~10 mm/s, and 1.5 cm×1.5 cm×1.5 cm cubic block samples are deposited layer by layer; (5) Then, the rotating speed of different powder conveying systems is adjusted to gradually increase the proportion of powder A and reduce the proportion of powder B in the mixed powder. According to different proportions, the laser power is gradually adjusted to deposit cubic block samples with different Nb content; (6) Step (5) is repeated continuously to prepare 20 block samples of nickel-based superalloy with 0~10 wt.% Nb content, as shown in figure 1.

Figure 1. Inconel 718 alloy block with different Nb contents manufactured by the high-throughput 3D-printing.

3. Results and Discussions

3.1. Nb Content Analysis of 3D Printed Inconel 718 Alloy

The theoretical and experimental values of Nb content in Inconel 718 alloy block at different rotational speeds were listed in table 1. The theoretical value is in good agreement with the experimental value, and the maximum error is only 0.15%. From figure 2, it can be found that the experimental and theoretical values of Nb content in Inconel 718 alloy block have a very good linear relationship with the rotational speed of A powder, and the corresponding R^2 is 0.998 and 1, respectively. The mathematical expressions are as follows:

$$y = a + bx$$

where, for the experimental value, a and b are -9.82 and 7.85 respectively; For the theoretical value, a and b are -9.93 and 7.98 respectively.

Table 1. The theoretical and experimental values of Nb content (wt.%) in Inconel 718 alloy block at different rotational speeds.

Sample number	Rotational speed of B powder	Rotational speed of A powder	Theoretical value	Experimental value	Error
1	0.00	0.70	1.03	1.03	0.00
2	0.03	0.67	1.33	1.28	0.05
3	0.06	0.64	1.63	1.62	0.01
4	0.09	0.61	1.92	1.85	0.07
5	0.12	0.58	2.22	2.08	0.14
6	0.15	0.55	2.52	2.43	0.09
7	0.18	0.52	2.82	2.73	0.09
8	0.21	0.49	3.11	3.02	0.09
9	0.24	0.46	3.41	3.30	0.11
10	0.27	0.43	3.71	3.60	0.11
11	0.30	0.40	4.01	3.93	0.08
12	0.33	0.37	4.31	4.24	0.07
13	0.36	0.34	4.60	4.50	0.10
14	0.39	0.31	4.90	4.79	0.11
15	0.42	0.28	5.20	5.10	0.10
16	0.45	0.25	5.50	5.40	0.10
17	0.48	0.22	5.80	5.70	0.10
18	0.51	0.19	6.09	5.94	0.15
19	0.54	0.16	6.39	6.26	0.13
20	0.57	0.13	6.69	6.65	0.04

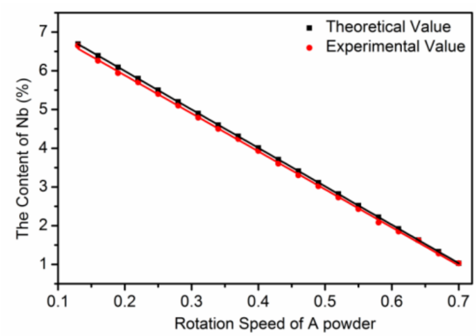

Figure 2. Trend of theoretical and experimental Nb content in 20 Inconel 718 alloy blocks with the variation of rotational speed of A powder.

3.2. Microstructure Analysis of 3D Printed Inconel 718 Alloy

Figure 3 shows the metallography of Inconel 718 alloy blocks with Nb content of 1.03 wt.%, 3.60 wt.% and 6.65 wt.%. Figure 4 displays the SEM morphology of Inconel 718 alloy block with same Nb content. It can be seen from two pictures that the high-throughput 3D-printed Inconel 718 alloy block not only has a large number of island-like Laves phase and massive carbide phase, but also has a small number of holes. With the increase of Nb content in the alloy, the content of Laves phase in the alloy increases gradually, and the Laves phase particles also become larger.

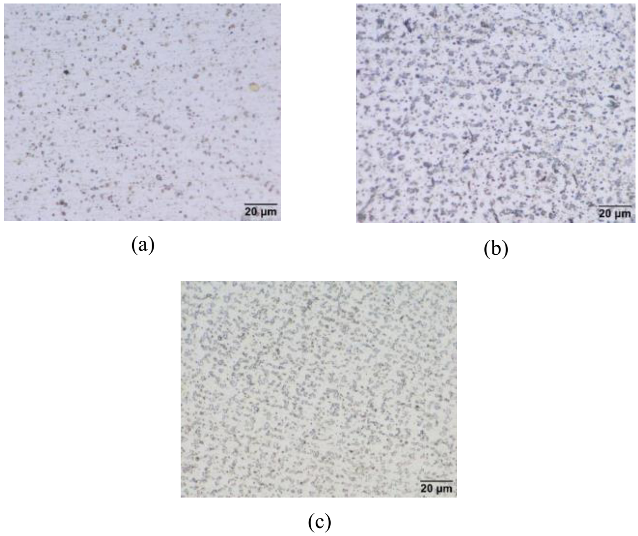

Figure 3. The metallography of Inconel 718 alloy blocks with Nb content of 1.03 wt.% (a), 3.60 wt.% (b) and 6.65 wt.% (c).

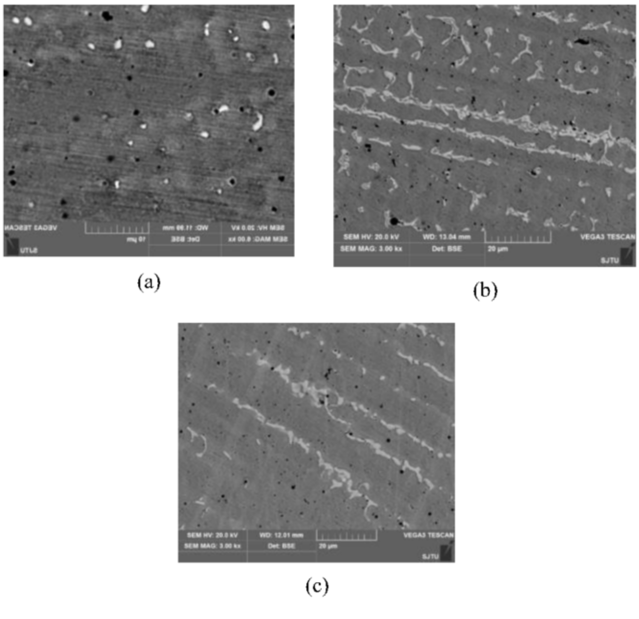

Figure 4. The SEM morphology of Inconel 718 alloy blocks with Nb content of 1.03 wt.% (a), 3.60 wt.% (b) and 6.65 wt.% (c).

3.3. The Hardness of 3D Printed Inconel 718 alloy

Figure 5(a) shows the hardness diagram of 20 Inconel 718 alloys. Three hardness points are selected for each sample. It can be seen that the general trend of hardness increases with the increase of Nb content in the alloy. Figure 5(b) shows the content of Laves phase in 20 Inconel 718 alloys. The horizontal and vertical sections of the sample are selected for statistics, and the variation trend is the same as the hardness. Combined with metallography and SEM, it can be seen that the Nb content in Inconel 718 alloy has a significant effect on the phase composition and Laves phase content of the alloy. Nb mainly exists in γ" (Ni_3Nb) and Laves phase [10-14]. With the increase of Nb content, the content of Laves phase in the alloy also increases. The Laves phase, γ phase and other precipitates in the alloy interact with each other to affect the hardness of the alloy [15].

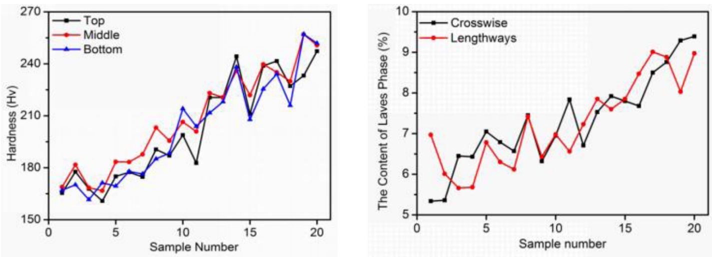

(a) (b)

Figure 5. Hardness trends at three points (a) and Laves phase content (b) in 20 Inconel 718 blocks.

4. Conclusions

In this study, 20 Inconel 718 samples with different Nb contents (0~10 wt.%) are prepared by high throughput method of additive manufacturing. Their microstructure and hardness are analyzed and several important conclusions are obtained. With the increase of Nb content in the alloy, the content of Laves phase in the alloy increases gradually, and the Laves phase particles also become larger. In addition, the Laves phase, γ phase and other precipitates in the alloy interact with each other to affect the hardness of the alloy.

Acknowledgment

This work is supported by the Technical Innovation Projects (Project Number 21SG-13).

References

[1] Kong DC, Dong CF, Ni XQ, Zhang L, Man C, Yao JZ, Ji YC, Ying YP, Xiao K, Cheng XQ and Li XG. High-throughput fabrication of nickel-based alloys with different Nb contents via a dual-feed additive manufacturing system: Effect of Nb content on microstructural and mechanical properties J. Alloys Compd. 2019; 785: 826-837

[2] Tarzimoghadam Z, Ponge D, Klower J and Raabe D. Hydrogen-assisted failure in Ni-based superalloy 718 studied under in situ hydrogen charging: The role of localized deformation in crack propagation. Acta Mater. 2017; 128: 365-374

[3] Zhu L, Xu ZF, Liu P and Gu YF. Effect of processing parameters on microstructure of laser solid forming Inconel 718 superalloy. Opt. Laser Technol. 2018; 98: 409-415

[4] Zhang Y, Song J, Yan LM, Shi SP and Peng SM. First principles calculation of redox potential for tetravalent actinides in molten LiCl-KCl eutectic based on vertical substitution and relaxation. Electrchim. Acta. 2019; 239: 466-475

[5] Song J, Wu WH, Zhang L, He BB, Lu L, Ni XQ, Long QL, Zhu GL. Role of scanning strategy on residual stress distribution in Ti-6Al-4V alloy prepared by selective laser melting. Optik. 2018; 170: 342-352

[6] Wang Z, Guan K, Gao M, Li X, Chen X and Zeng X. The microstructure and mechanical properties of deposited-IN718 by selective laser melting. J. Alloys Compd. 2012; 513: 518-523

[7] Kong DC, Dong CF, Ni XQ, Zhang L, Man C, Zhu G, Yao JZ, Wang L, Cheng XQ and Li XG. Effect of TiC content on the mechanical and corrosion properties of Inconel 718 alloy facricated by a high-throughput dual-feed laser metal deposition system. J. Alloys Compd. 2019; 803: 637-648

[8] Parry LA, Ashcroft IA and Wildman RD. Geometrical effects on residual stress in selective laser melting. Addit. Manuf. 2019; 25: 166-175

[9] Song J, Zhang L, Wu WH, He BB and Lu L. Understanding processing parameters affecting residual stress in selective laser melting of Inconel 718 through numerical modeling. J. Mater. Res. 2019; 34: 1395-1404

[10] Lawitzki R, Hassan S, Karge L, Wagner J, Wang D, Kobylinski JV, Krempaszky C, Hofmann M, Gilles R and Schmitz G. Differentiation of γ'-and γ''-precipitates in Inconel 718 by a complementary study with small-angle neutron scattering and analytical microscopy. Acta Mater. 2019; 163: 28-39

[11] Zhang F, Levine LE, Allen AJ, Stoudt MR, Lindwall G, Lass EA, Williams ME, Idell Y and Campbell CE. Effect of heat treatment on the microstructural evolution of a nickel-based superalloy additive-manufactured by laser powder bed fusion. Acta Mater. 2018; 152: 200-214

[12] Song J, Li XJ, Yan LM, Jiang T and Shi SP. Towards the calculations of redox potentials in molten LiCl-KCl eutectic by ensemble averages based on first principles molecular dynamics. Electrochim. Acta. 2017; 248: 462-469

[13] Fayman FC. Microstructural characterization and elemental partitioning in a direct-aged superalloy (DA 718). Mater. Sci. Eng. 1987; 92: 159-171

[14] Devaux A, Nazé L, Molins R, Pineau A, Organista A, Guédou JY, Uginet JF and Héritier P. Gamma double prime precipitation kinetic in Alloy 718. Mater. Sci. Eng. 2008; 486: 117-122

[15] Li J, Zhao Z, Hai P, Qu H, Li L, Wu L, Guan R, Liu H and Guo Z. Microstructural evolution and mechanical properties of IN718 alloy fabricated by selective laser melting following different heat treatments. J. Alloys Compd. 2019; 772: 861-870